

Permutation Symmetry Restoration in Disordered Materials

Varda F. Hagh*

*Department of Mechanical Science and Engineering
University of Illinois Urbana-Champaign,
Urbana, IL 61801, USA.*

Sidney R. Nagel

*Department of Physics and The James Franck and Enrico Fermi Institutes
The University of Chicago, Chicago, IL 60637, USA.*

(Dated: March 7, 2024)

A disordered solid, such as an athermal jammed packing of soft spheres exists in a rugged potential-energy landscape in which there are a myriad of stable configurations that defy easy enumeration and characterization. Nevertheless, in three-dimensional monodisperse particle packings, we find an astonishing regularity in the distribution of basin volumes, V_{Nd} , as measured by their frequency of occurrence in a random sampling algorithm. Ordering the basins according to their size, from the largest at $n = 1$, to the smallest, we find approximately that $V_{Nd} \propto n^{-1}$. This statistical regularity persists up to the largest systems for which we can collect sufficient data. In monodisperse packings there is “permutation symmetry” since identical particles can always be interchanged without affecting the system or its properties. Introducing any polydispersity breaks this symmetry and leads to a proliferation of distinct configurations. We present an algorithm that partially restores permutation symmetry to such polydisperse packings.

A collection of N soft particles can be packed into a box in a multitude of ways that can be accessed either by randomizing the initial particle positions or by imposing deformations that lead to particle rearrangements. In d -dimensions, the Nd -dimensional potential-energy landscape consists of basins whose minima each correspond to a single mechanically-stable configuration. Those energy basins with larger volume, V_{Nd} , have a higher probability of being found when the system is sampled randomly [1–6]. As N , d , or other physical degrees of freedom such as particle shape or polydispersity increase, the number of distinct stable arrangements, n_p , grows rapidly. In general, it is rare to land in one configuration repeatedly unless the system is exceedingly small as was demonstrated in $d = 2$ for $N \leq 16$ bidisperse disks where Xu et al. were able to find a significant fraction of the n_p stable configurations [3, 5]. The conclusion from that work was that the distribution of basin volumes followed a log-normal distribution around an average basin size. As N increases, each basin occupies a smaller and smaller fraction of the entire configuration space.

In this paper, we study the configurations of *monodisperse* systems in $d = 3$ created by minimizing the system’s potential energy after starting from randomly chosen initial particle positions. Here, the same configurations are repeatedly found for small N . However, the number found is much smaller than in the bidisperse $d = 2$ systems because, for monodisperse packings, the identical particles can be permuted without changing the packing. The extra states added by permutations in a

bidisperse (and more generally in a polydisperse) system overwhelm the number of intrinsic ground states of the monodisperse system [7]. Here we introduce a new protocol that allows permutation symmetry to be partially restored in a polydisperse system. This allows us to investigate the relationship of polydisperse packings to those which are monodisperse. We examine both the distribution of basin volumes and the role of polydispersity.

The monodisperse landscape: We first investigate monodisperse soft-sphere systems in $d = 3$. We use harmonic interactions between particles i and j with radii R_i and R_j located at positions \mathbf{r}_i and \mathbf{r}_j :

$$E_{i,j} = \sum_{i,j} \epsilon_0 \left(1 - \frac{|\mathbf{r}_i - \mathbf{r}_j|}{R_i + R_j}\right)^2 \Theta \left(1 - \frac{|\mathbf{r}_i - \mathbf{r}_j|}{R_i + R_j}\right), \quad (1)$$

where ϵ_0 is a constant setting the scale of the energy, $\Theta(x)$ is the Heaviside step function, and $R_i = R_j = R$ when the packings are monodisperse. We study packing fractions $0.70 < \phi < 0.85$ with the number of particles $13 < N < 293$. In all of our studies of the monodisperse landscape, we sample an ensemble of 10^6 randomly chosen initial conditions (that is we choose random numbers for each coordinate of each particle). We minimize the energy of each configuration to quad precision using a GPU based implementation of the FIRE algorithm [8]. We determine whether two initial configurations end in the same state by comparing the energies of minimized states. If they are the same to 32 decimal places we then check to see if their connectivity is the same. That is we check that modulo particle labeling, the particles have the same connections. There are some symmetries, for example, reflections, rotations by 90° in a square box, and rigid translations, that we *do not* count as distinct.

* hagh@illinois.edu

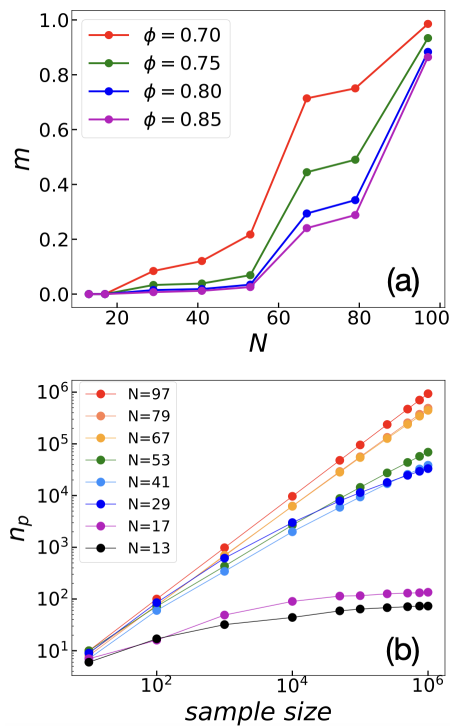


FIG. 1. (a) The fraction of distinct stable configurations, m , found in 10^6 random samples of $d = 3$ monodisperse packings versus system size, N . Below $N = 50$, relatively few stable states are found. As N increases, the fraction of new states found proliferates rapidly. At the four packing fractions, ϕ , shown in the legend, m decreases with increasing the packing fraction. (b) The number of distinct stable configurations, n_p , versus the number of trials (random initial conditions) at packing fraction $\phi = 0.75$ for different size systems, N . At small N , n_p saturates while at large N , only a few states are found more than once.

Our results are illustrated in Fig. 1a. We use m to show the fraction of distinct stable configurations in an ensemble. For small size, $N = 13$, the number of distinct configurations, n_p , when the landscape is randomly sampled one million times (*i.e.* $m = \frac{n_p}{10^6}$), is fewer than 105 for all densities studied. For $N = 17$, the number grows to ≈ 220 at $\phi = 0.70$ which is the lowest density we study. As the packing fraction ϕ increases, there is a decrease in the number of distinct configurations. This is because closer to the jamming threshold the system becomes particularly sensitive to perturbations. Even a small displacement can trigger significant rearrangements and lead to a new configuration, resulting in a more rugged and complex landscape [9, 10]. The structure of data in Fig. 1a shows a consistent trend: as ϕ increases, some of the basins disappear.

The number of distinct stable configurations, n_p , grows rapidly with increasing system size, N . As N increases above $N = 50$, n_p rises sharply until it begins to approach 10^6 , resulting in $m \rightarrow 1$. In Fig. 1b, we show n_p as a function of sampling ensemble size at $\phi = 0.75$. For

systems with $N \leq 17$, the curves quickly reach a plateau suggesting that we are effectively exploring nearly all the available basins. For larger N , the curves show hardly any saturation; new, un-visited configurations continue to be found at nearly the same rate as they were at the start. These results, especially at large N , show that 10^6 trials is not an exhaustive sampling of all the basins. For example, for $N = 293$ at $\phi = 0.75$, only 5 out of one million trials landed in a previously discovered basin. The sheer enormity of the number of basins results in only a minute fraction of configurations falling into the same basin multiple times [11].

Statistical order in the monodisperse landscape: The data in Fig. 1 suggest that the basins must have very different volumes, V_{Nd} , because some configurations are found repeatedly while others are found only once or not at all. This was also noted in the $d = 2$ studies of bidisperse systems [3, 5]. In order to explore this variation, we rank the basin volumes in descending order: $n = 1$ is the largest basin which has been found the most times; $n = 2$ is the second largest basin, *etc.* In Fig. 2, we plot the probability, $P(n)$, that the n th basin would be found versus n . $P(n)$ is the total number of times a basis was found divided by the number of trials, which is 10^6 for monodisperse packings. By construction, this must be a monotonically decreasing function. For clarity, we split the results into two bins: Fig. 2a, shows the results for $N < 50$ and Fig. 2b shows the results for $N > 50$.

For the larger system sizes ($N > 50$) shown in Fig. 2b, $P(n)$ appears to approach a simple scaling behavior: $P(n) \propto n^{-\beta}$ with $\beta \approx 1.0 \pm 0.1$. We note that there are detectable deviations from the straight-line behavior on these graphs. Nevertheless, the overall trends are very clear. For large n , the trend is cut off by the number of samples in our ensemble, *i.e.*, 10^6 . This behavior persists out to the largest system size we investigated: $N = 293$. In Fig. 2c, we show the data as a function of packing fraction, ϕ , for a single system size ($N=97$). The variation with ϕ does not alter the scaling behavior and only shifts the prefactor.

In the smaller systems ($N < 50$) shown in Fig. 2a, this scaling is truncated. We therefore try fitting each data set by a power-law cut off by an exponential factor: $P(n) \propto \frac{1}{n} e^{-n/n_0}$, with n_0 representing a cutoff that grows with system size. The inset shows n_0 versus N . For $N > 50$, the value of n_0 becomes too large to be extracted from our data and the simple scaling $P(n) \propto n^{-\beta}$ is a good description of the data. While our data show that $\beta \approx 1.0 \pm 0.1$, we are unable to determine if there are slight variations in its value as a function of N or ϕ .

These results were for monodisperse systems in $d = 3$. Any polydispersity would have made it computationally prohibitive to search for identical stable configurations. Even for our smallest systems, the $N!$ different permutations of the particles far exceeds our capabilities. Our results make it clear that if there is permutation symmetry (*i.e.*, that particles can be permuted in any order – amounting only to relabeling the particles – without

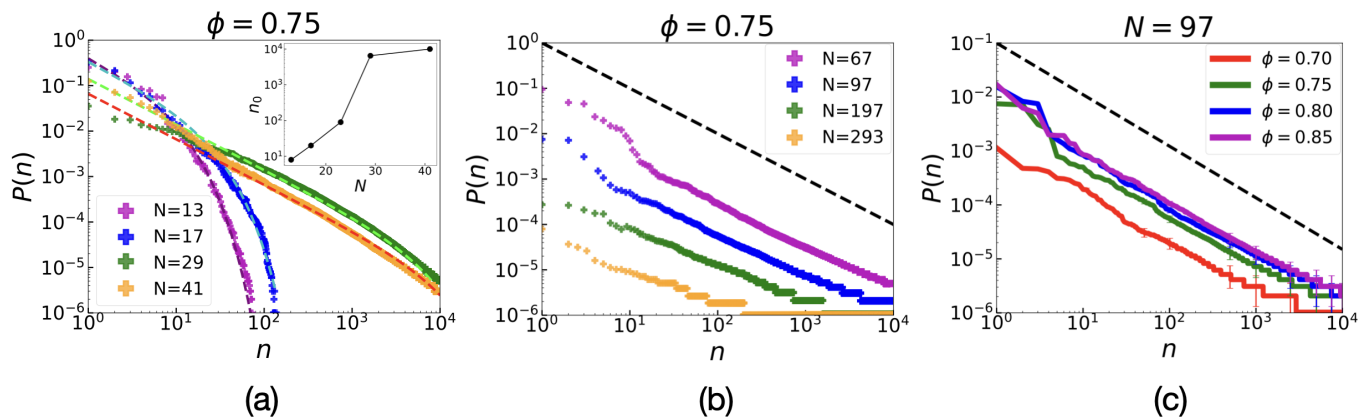


FIG. 2. (a) The probability of finding a basin, P , versus the rank order, n , of basin sizes in 10^6 randomly sampled monodisperse packings of $N = 13, 17, 29$, and 41 particles at $\phi = 0.75$. The dashed lines are fits to: $\frac{1}{n}e^{-n/n_0}$. The inset shows n_0 versus N . (b) Same as (a) for larger system sizes: $N = 67, 97, 197$, and 293 at $\phi = 0.75$. The black dashed line, a guide to the eye, has slope -1 . Even for $N = 293$, there are nearly 2 decades of approximately power-law behavior. (c) The probability for packings with $N = 97$ particles at four different packing fraction values. The black dashed line, a guide to the eye, has slope -1 .

affecting the system), the number of distinct states is far less than we naively expected. In this case, the underlying structure of the packings can be made manifest so that surprising statistical order emerges.

Breaking – and partial restoration of – permutation symmetry: Breaking permutation symmetry by introducing small amounts of polydispersity results in an enormous increase in the number of distinct minima in the energy landscape. Even for our smallest system, $N = 13$, any polydispersity makes it impossible for us to access the same state twice by random sampling of initial conditions.

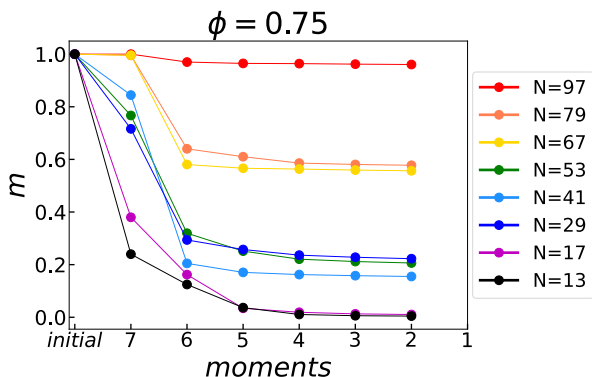


FIG. 3. The fraction of distinct stable configurations in 10^4 random samples of packing fraction $\phi = 0.75$ and polydispersity $\sigma = 0.01$ as a function of moments of radii that are constrained during minimization for various system sizes.

However, if the degree of polydispersity is small, a single large basin in the monodisperse case will disappear and be replaced by a set of smaller basins – one for each permutation of the particles. Some traits of the large monodisperse basin can be detected in the individual off-spring. Thus, despite the enormous effect of polydispersity

on breaking the permutation symmetry, the addition of very small amounts of polydispersity can nevertheless be viewed as a perturbation to monodisperse packings.

In order to see this, we apply the following algorithm to partially “restore” the permutation symmetry. We create an ensemble of N polydisperse spheres; each sphere has a different radius chosen from a log-normal distribution of particle sizes of width σ_R and mean $\langle R \rangle$. We define polydispersity as $\sigma = \frac{\sigma_R}{\langle R \rangle}$. Once these radii have been chosen, we use the same set of radii for each random configuration in the ensemble. We then minimize the total energy of the system. To lower the energy, in addition to moving the particle positions we also allow the particle radii to change [12]. This process is reminiscent of the swap Monte Carlo [13–16], but instead of doing individual swaps between particles of different sizes, we let all radii adjust simultaneously (more similar to collective swap algorithms [17, 18]). In this process, the radii are considered as variables. However, unrestricted changes in radii can significantly change their distribution, potentially causing some radii to go to zero and un-jam the system. To circumvent this, we constrain certain moments of the distribution by removing components of radii forces, $\frac{\partial E}{\partial R_i}$, perpendicular to the $\sum_i R_i^\alpha = c$ plane where c is a constant. Initially, we fix seven moments $\alpha = (-6, -3, -1, 1, 2, 3, 6)$, maintaining the radii distribution close to the original while enhancing stability [12]. The choice of seven initial moments is arbitrary, as it only should ensure stability of packings without any un-jamming. In the final stage of the protocol, we replace the output of the radii minimization procedure with the *original* particle radii. We do this based on their size ranking: the largest particle in the radii-minimized configuration is replaced with the largest original particle, then we do the same for the next largest particle *etc.* until we have replaced all the particles. Finally, we minimize the energy one more time (without allowing the radii to change

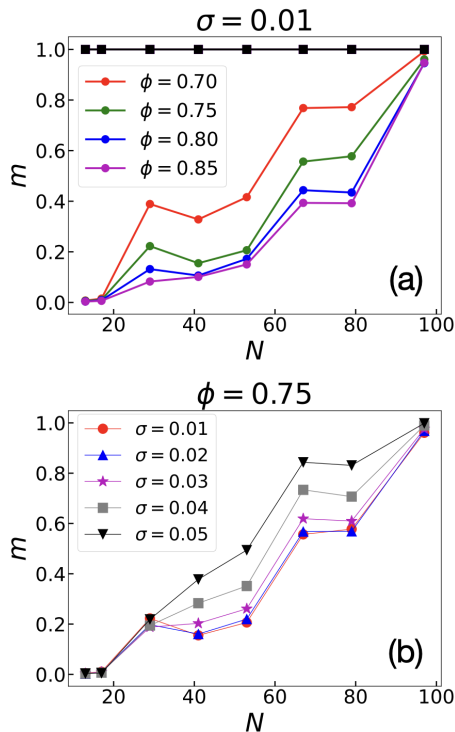


FIG. 4. (a) The fraction of distinct polydisperse packings in 10^4 samples as a function of system size and packing fraction. Black square markers represent the fraction of distinct packings in a random sampling of the landscape when there is 1% polydispersity. Circle markers show the fractions after applying the retrieval algorithm. (b) The fraction of distinct stable configurations after applying the retrieval algorithm as a function of polydispersity and size for an ensemble of 10^4 packings at $\phi = 0.75$.

during this final minimization) since slight changes in particle sizes could take the system out of equilibrium.

By going through this cycle of (i) energy minimization with respect to radii and positions, (ii) radii replacement, and then (iii) energy minimization with respect to positions, we obtain a decrease in the fraction of distinct packings. Following this, we repeat the minimization, this time constraining only six out of the initial seven moments of the radii distribution. The process continues, progressively reducing the number of fixed moments during radii minimization and replacing the resulting radii with equivalent values from the original packing. The fraction of distinct packings decreases as we decrease the number of moments. We continue reducing the number of fixed moments until we constrain only two moments, $\alpha = \{-3, 3\}$, during minimization. Two is the minimum number of constraints required to keep all packings jammed across various sizes and packing fractions. This procedure yields an ultra-stable version of the original set of particles.

This process vastly reduces the number of distinct packings as depicted in Fig. 3. Whereas the original polydisperse sample never recovered the same configura-

tion twice, the samples with particle replacements after the minimization with position and radii ended up in the same basins multiple times as shown in Fig. 4a for various packing fractions and in Fig. 4b for different polydispersities, σ .

The notable decrease in the fraction of distinct packings following this procedure is intriguing. Although these minima are initially distinct, in the end, they cluster into a relatively few local basins; radii minimization funnels many states into the same deep minimum. Remarkably, even at polydispersities up to 5%, the fraction m after radii minimization and replacement is small. This decrease is evident across various polydispersity values but becomes less pronounced for larger polydispersities in larger system sizes. Fig. 4b shows the fraction of distinct packings after applying our algorithm to packing sets with various polydispersity values at a packing fraction of $\phi = 0.75$.

To gain deeper insight into the distribution of these repeated basins on the polydisperse landscape and to evaluate if they conform to the statistical regularity of the monodisperse landscape, we examine the probability of finding each basin against its frequency rank, as illustrated in Fig. 5; the probability scales inversely with the rank n , reminiscent of the monodisperse landscape shown in Fig. 2. A crucial question is whether these repeated minima are truly similar to the large basins that existed on the monodisperse landscape. To investigate this, we set the radii of the polydisperse packings in these distinct minima to the monodisperse value while fixing the packing fraction and then equilibrate them with respect to positional degrees of freedom only. We find that all packings clustered into the same basins on the polydisperse landscape end up in one of the previously observed larger basins on the monodisperse landscape. This holds true for all studied polydispersity values, whether decreased to zero abruptly or gradually. Fig. 6 illustrates this for packings that are shifted to monodispersity in a single step. The black data show the equivalent fractions of random monodisperse packings. This figure demonstrates that our algorithm partially retrieves permutation symmetry in the polydisperse landscape.

Discussion: The presence of permutation symmetry in disordered arrangements of soft particles results in a drastic reduction in the number of stable configurations available to the system. For monodisperse packings with sizes $N \leq 17$, the number of distinct minima, n_p identified through randomly sampling the landscape a million times in densities $0.70 < \phi < 0.85$ is in the range $33 < n_p < 220$. The introduction of a small amount of polydispersity to the system breaks the permutation symmetry, leading to an enormous increase in the number of available basins. Even after ten thousand landscape samplings, no minimum is visited twice. This highlights the impact of polydispersity on the number of basins in the landscape.

Our results show that by identifying the exceptionally deep minima associated with ultra-stable packings in the

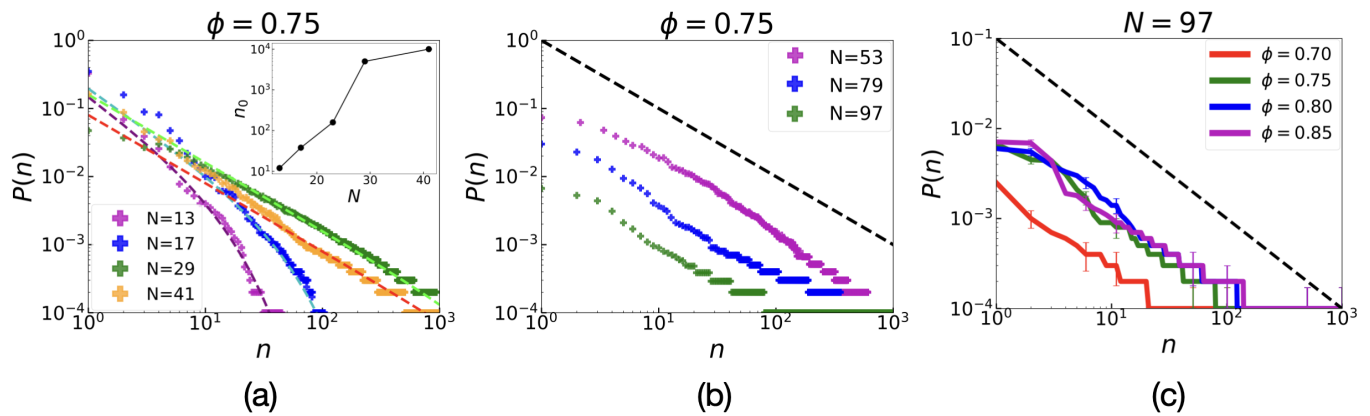


FIG. 5. The probability of finding a basin as a function of the rank ordering of basin sizes, in 10^4 polydisperse packings after they have been processed through the algorithm with two moments of distribution being constrained. (a) The probability for packings with $N = 13, 17, 29,$ and 41 particles at $\phi = 0.75$. The dashed lines indicate a fitted curve of the form $\frac{1}{n} e^{-n/n_0}$. The inset shows how n_0 grows with system size. (b) The probability for packings with $N = 53, 79,$ and 97 , particles at $\phi = 0.75$. The black dashed line has slope -1 and is plotted to guide the eye. (c) The probability for packings with $N = 97$ particles at four different packing fraction values. The black dashed line has slope -1 and is plotted to guide the eye.

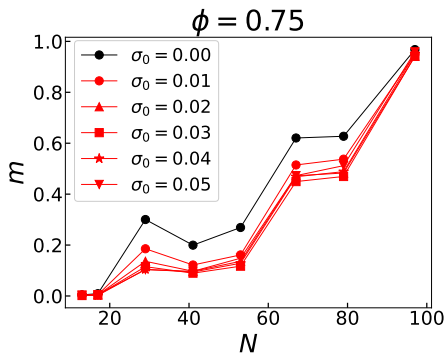


FIG. 6. The fraction of distinct stable configurations in 10^4 monodisperse packings produced randomly (black) and by replacing all radii in the polydisperse packings of various initial polydispersity values, σ_0 , with one value such that the packing fraction is fixed at $\phi = 0.75$ (red) as a function of system size. The polydisperse packings corresponding to red markers are the packings shown in Fig. 4b

polydisperse landscape, we can recover the ordered patterns present in the monodisperse system due to permutation symmetry. This not only produces a drastic

reduction in the number of distinct minima but also produces the statistical regularity of how the basin volumes are distributed. We believe that this remarkable regularity must have many consequences for the properties of glasses and jammed solids.

Generally, breaking physical symmetries in particle systems can introduce disorder by rendering the landscape more rugged. In the present study, we have shown that we can partially restore an important symmetry: permutation of the particles. This allows us to find the stable configurations that reflect the vastly simpler landscape of the monodisperse system. This finding is important in its own right because it also indicates how various methods, such as swap Monte-Carlo [13–16], based on the swapping of different-size particles, can be related to the physics of a monodisperse amorphous solid. We thank Eric Corwin and Thomas Witten for fruitful discussions. SRN was supported by the University of Chicago Materials Research Science and Engineering Center, NSF-MRSEC program under award NSF-DMR 2011854. VFH was supported by the US Department of Energy, Office of Science, Basic Energy Sciences, under Grant DE-SC0020972.

-
- [1] C. S. O’Hern, S. A. Langer, A. J. Liu, and S. R. Nagel, *Physical Review Letters* **88**, 075507 (2002).
 [2] C. S. O’Hern, L. E. Silbert, A. J. Liu, and S. R. Nagel, *Physical Review E* **68**, 011306 (2003).
 [3] N. Xu, J. Blawdziewicz, and C. S. O’Hern, *Physical Review E* **71**, 061306 (2005).
 [4] J. P. Doye and C. P. Massen, *The Journal of chemical physics* **122** (2005).
 [5] N. Xu, D. Frenkel, and A. J. Liu, *Physical Review Letters* **106**, 245502 (2011).
 [6] D. Frenkel, D. Asenjo, and F. Paillusson, *Molecular Physics* **111**, 3641 (2013).
 [7] M. Ozawa, G. Parisi, and L. Berthier, *The Journal of Chemical Physics* **149** (2018).
 [8] P. K. Morse and E. I. Corwin, *Physical review letters* **112**, 115701 (2014).
 [9] R. Dennis and E. Corwin, *Physical review letters* **124**, 078002 (2020).

- [10] C. Artiago, P. Baldan, and G. Parisi, *Physical Review E* **101**, 052605 (2020).
- [11] S. Martiniani, K. J. Schrenk, J. D. Stevenson, D. J. Wales, and D. Frenkel, *Physical Review E* **93**, 012906 (2016).
- [12] V. F. Hagh, S. R. Nagel, A. J. Liu, M. L. Manning, and E. I. Corwin, *Proceedings of the National Academy of Sciences* **119**, e2117622119 (2022).
- [13] A. Ninarello, L. Berthier, and D. Coslovich, *Physical Review X* **7**, 021039 (2017).
- [14] H. Ikeda, F. Zamponi, and A. Ikeda, *The Journal of chemical physics* **147** (2017).
- [15] C. Brito, E. Lerner, and M. Wyart, *Physical Review X* **8**, 031050 (2018).
- [16] L. Berthier, E. Flenner, C. J. Fullerton, C. Scalliet, and M. Singh, *Journal of Statistical Mechanics: Theory and Experiment* **2019**, 064004 (2019).
- [17] F. Ghimentì, L. Berthier, and F. van Wijland, *arXiv preprint arXiv:2402.06585* (2024).
- [18] S. Kim and S. Hilgenfeldt, *arXiv preprint arXiv:2402.08390* (2024).